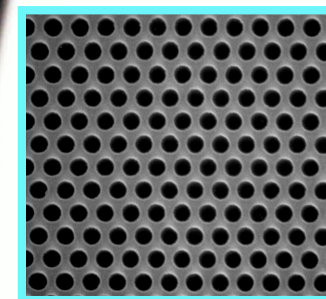
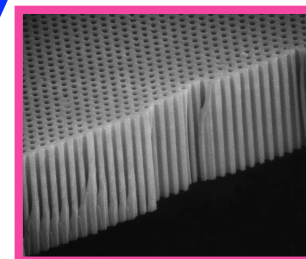
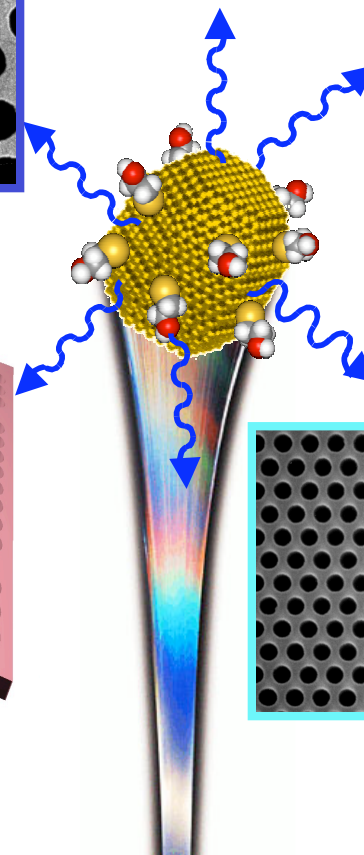
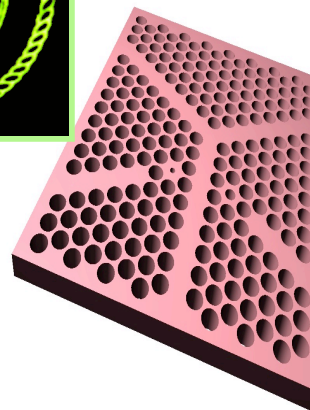
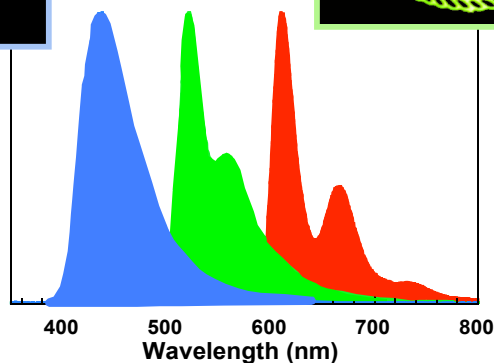
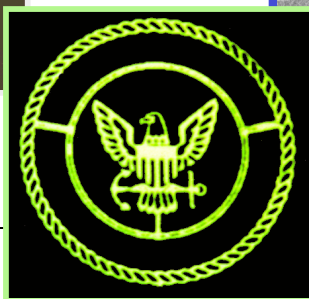
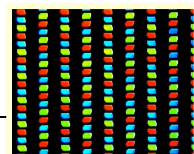
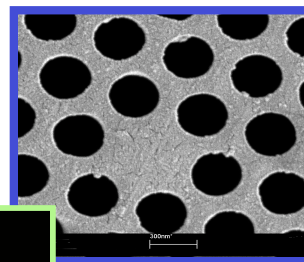
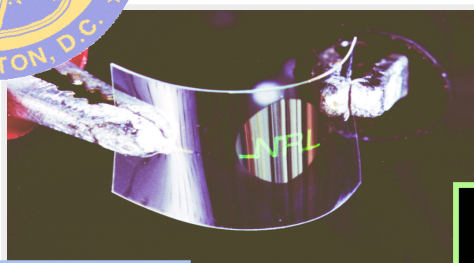
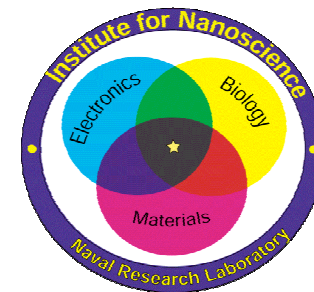




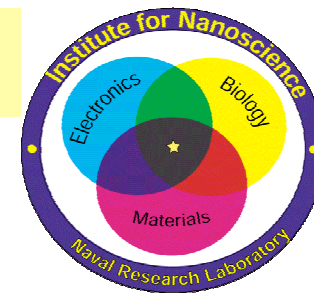
NANOSCIENCE RESEARCH IN OPTICS



Zakya H. Kafafi
Head, Organic Optoelectronics Section
Naval Research Laboratory, Washington, D.C. 20375
Phone/facsimile: 202-767-9529/404-8114
E-mail: kafafi@ccf.nrl.navy.mil

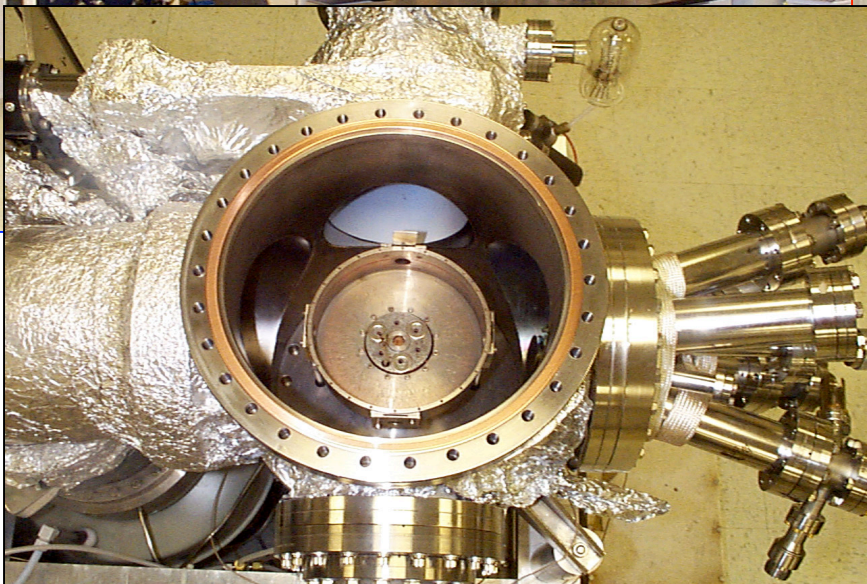


RESEARCH FACILITIES IN OPTICS



Synthetic Chemistry

Optical & Device
Characterization

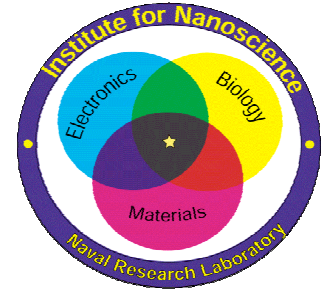


Top View of the Multi-surface
Vacuum Deposition Apparatus

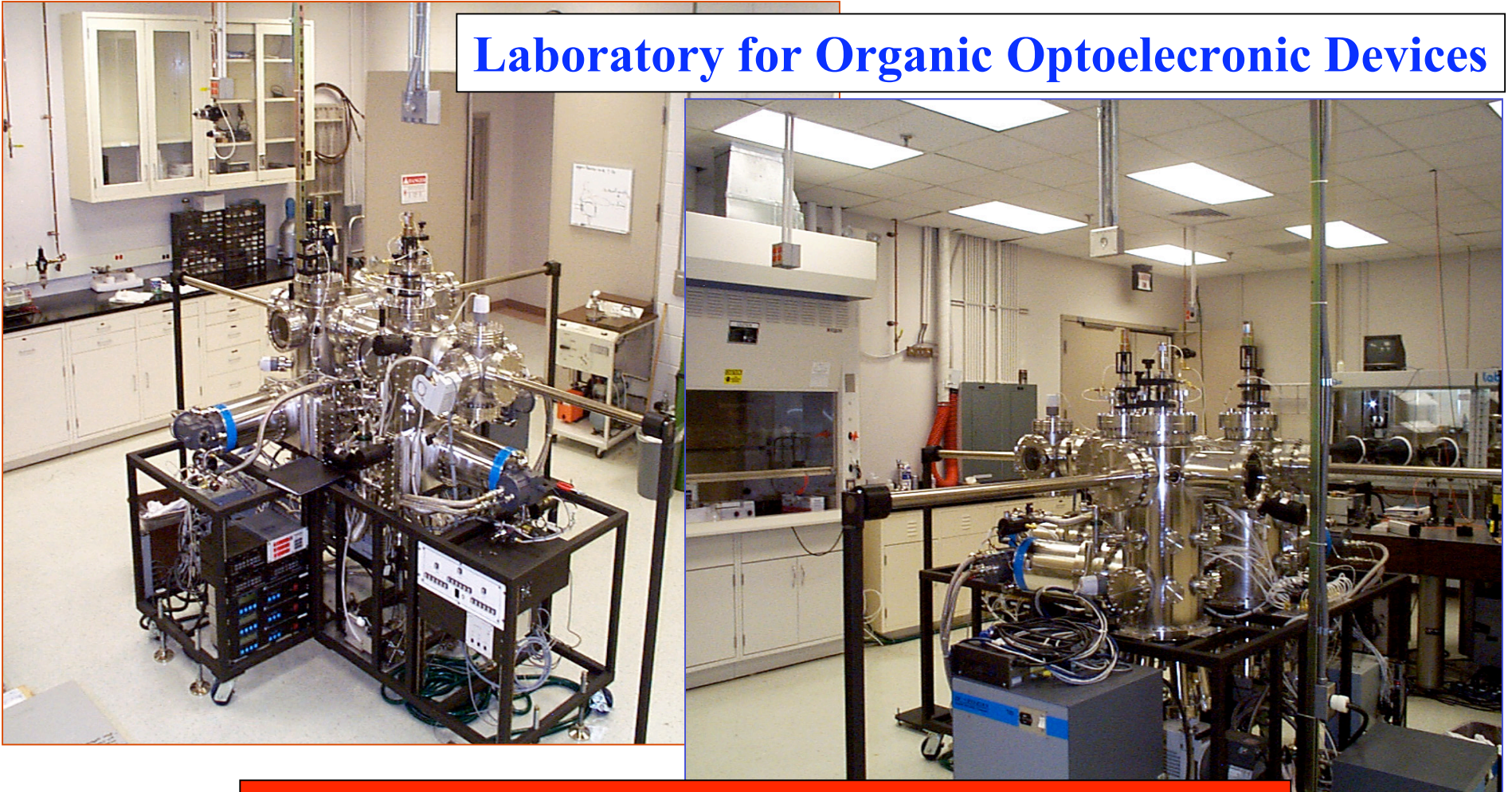




RESEARCH FACILITIES IN OPTICS



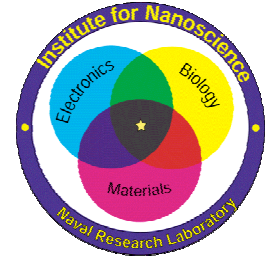
Laboratory for Organic Optoelectronic Devices



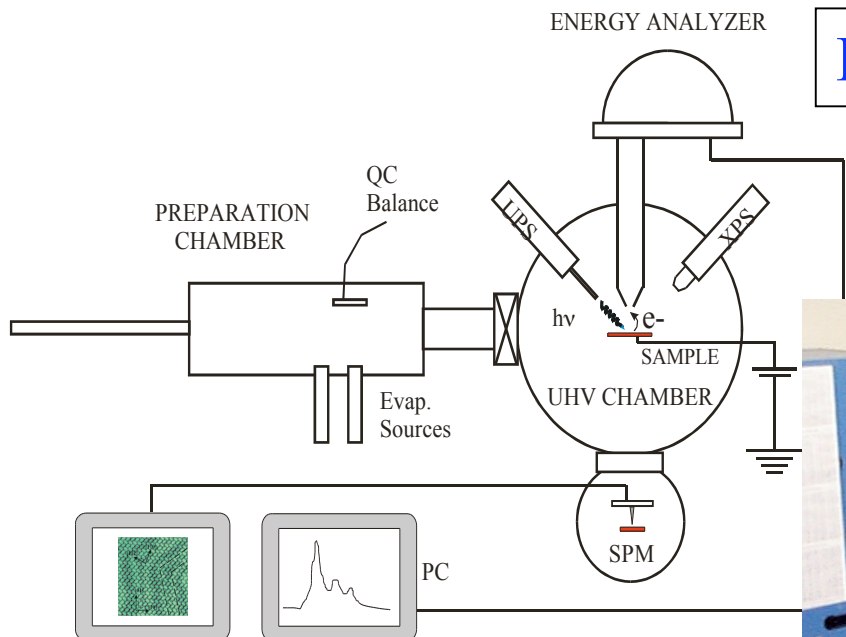
Multi-chamber Vacuum Deposition Apparatus



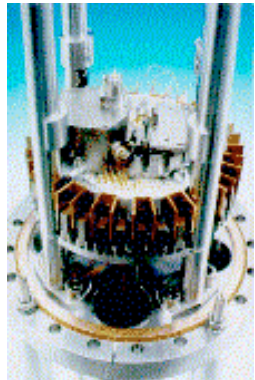
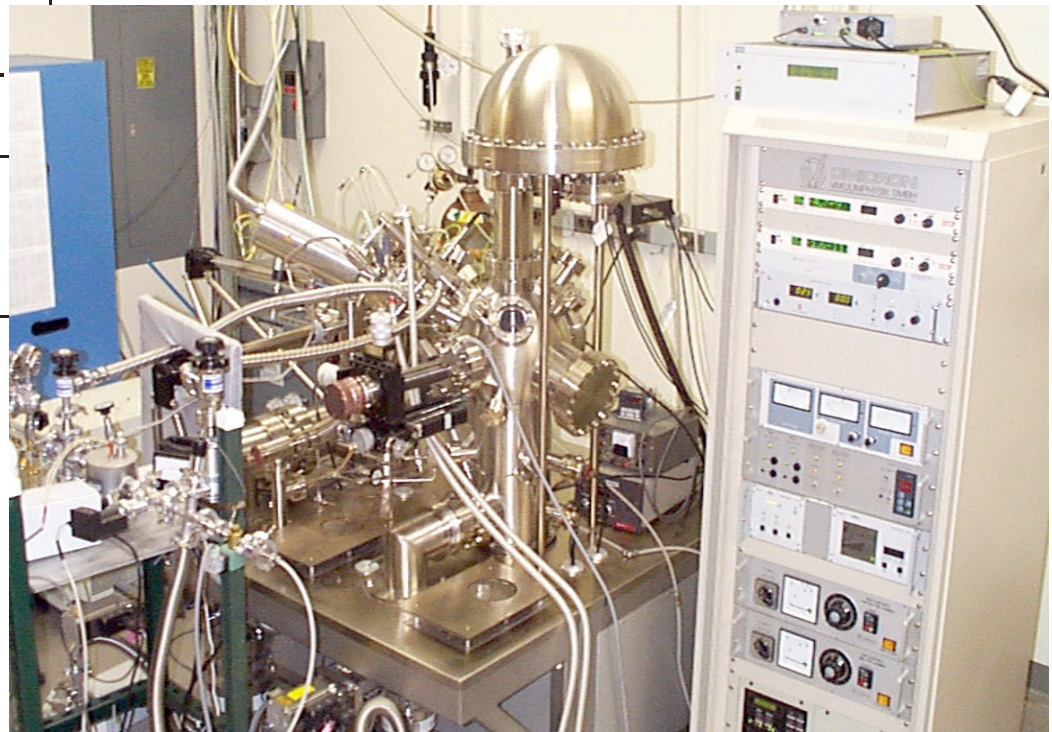
RESEARCH FACILITIES IN OPTICS



Laboratory for Surface Science



UPS / XPS / AFM / STM



Omicron AFM/STM

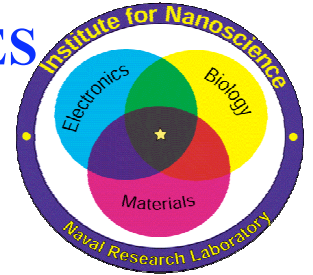
Omicron Multiprobe XP



ORGANIC LIGHT-EMITTING MATERIALS & DEVICES

Zakya H. Kafafi

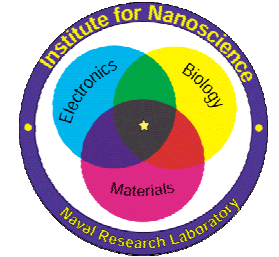
E-mail: kafafi@ccf.nrl.navy.mil



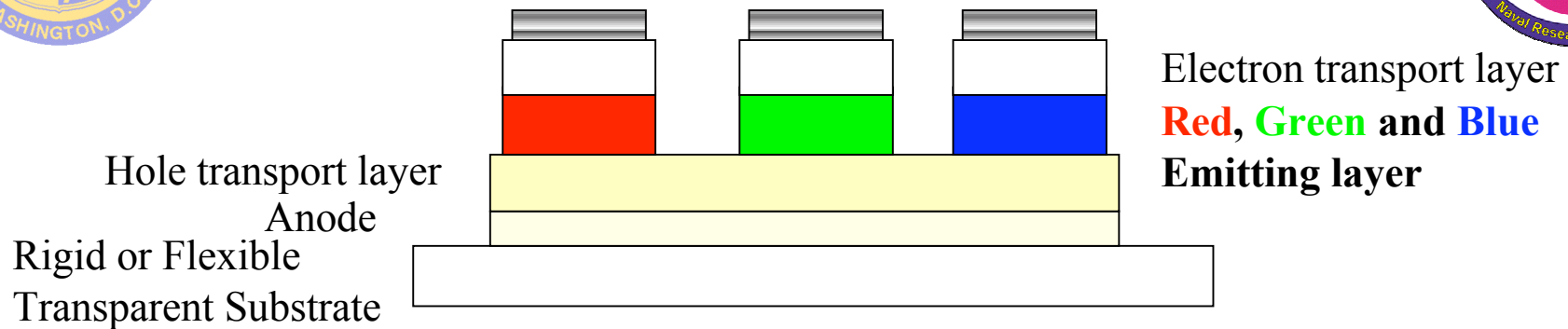
Objective: Develop the science base for thermally-stable, long-living, multi-colored, highly-efficient, organic light-emitting displays



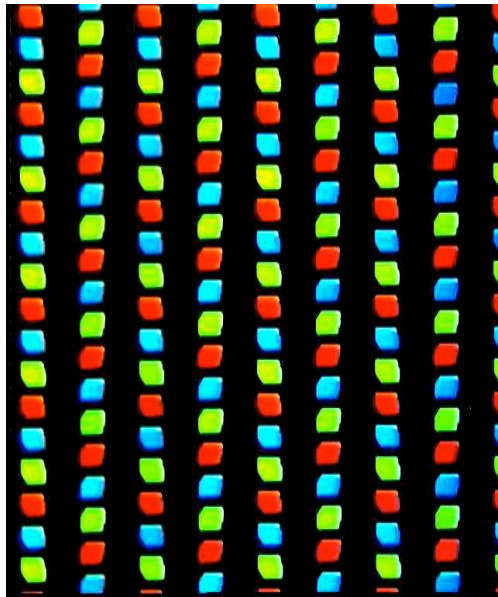
Impact: Command & control centers; maps & battle field simulators; helmet mounted displays; tank & aircraft cockpit displays; portable computers & communications



Organic Light-Emitting Pixel



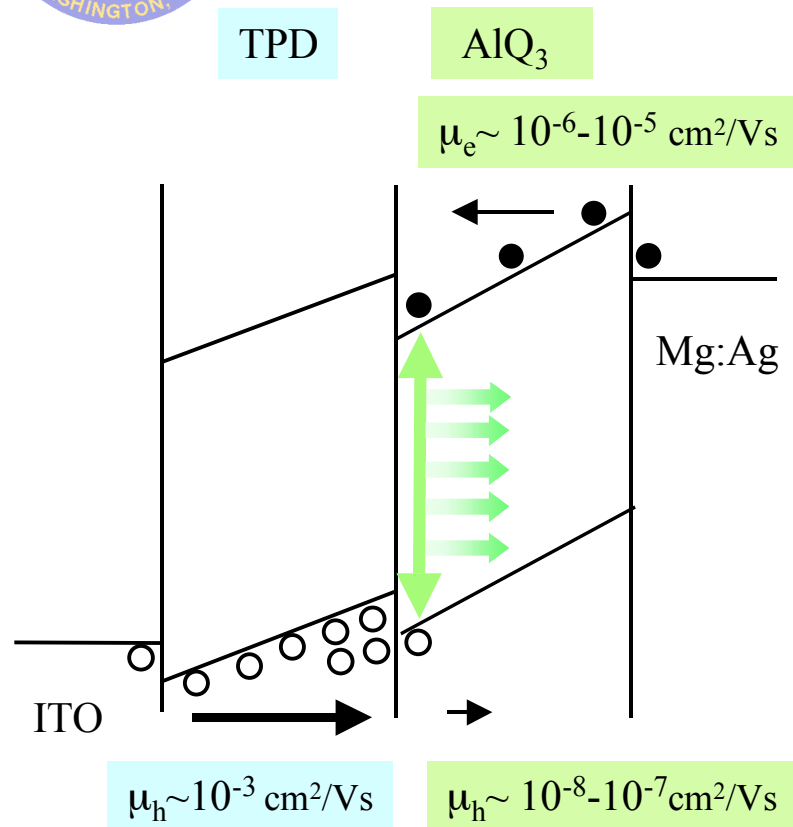
ADVANTAGES



- Rigid or flexible, thin and very light-weight displays
- Self-emissive (*no need for high-powered backlight*)
- Color tunable (*achieved by molecular engineering*)
- Extremely bright displays (*not susceptible to sunlight washout*)
- Sunlight readable and dimmable for night vision
- High durability (*lifetime >10,000 hrs @ 300 cd/m²*)
- Wide operating temperature (*-150 °C to 200 °C*) range
- Excellent viewing angle (*>170° with no loss in brightness*)
- High resolution (*pixel size as small as 12 μm or smaller*)



Control Device based on TPD/Alq₃ Heterostructure

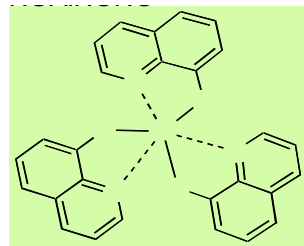
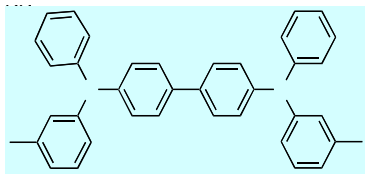


Important Issues

- Efficient electron injection
- Improved electron transport
- High solid state PL quantum yield

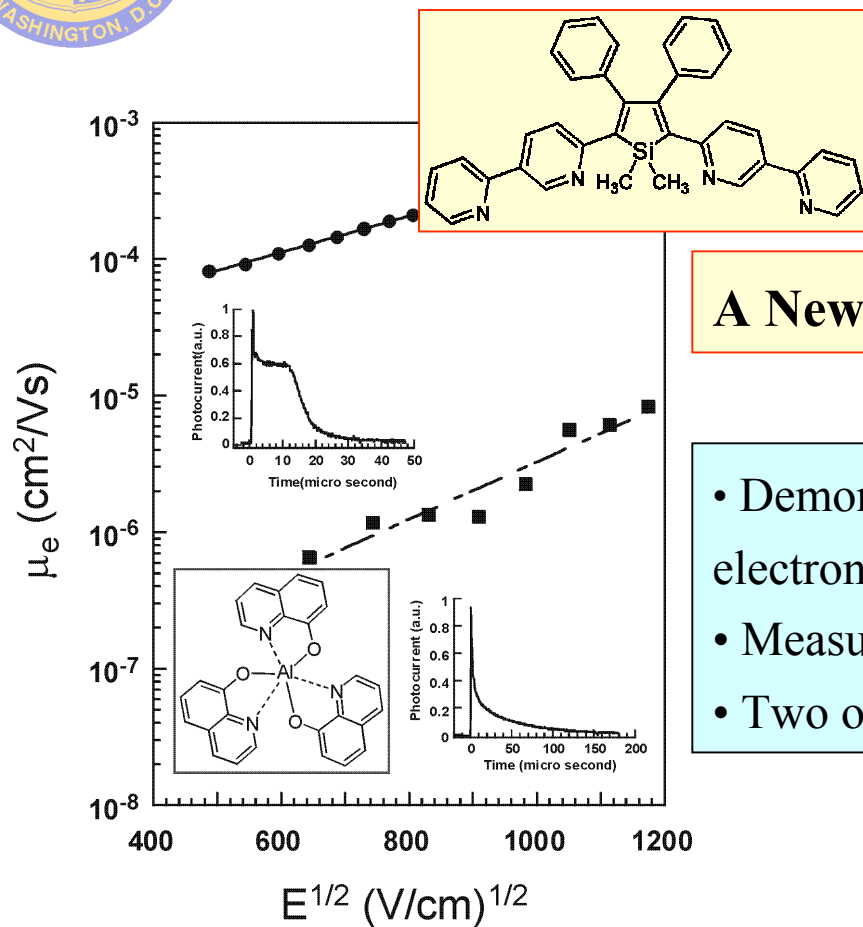
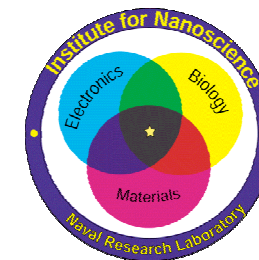
$$\eta_{EL} = \alpha \gamma \eta_r \phi_{PL}$$

- α : Light output coupling factor $\sim 1/2n^2$
- γ : Probability of carrier recombination
- η_r : Production efficiency of excitons
- ϕ_{PL} : Photoluminescence quantum yield





Novel Electron Transporters Based on Silole Derivatives



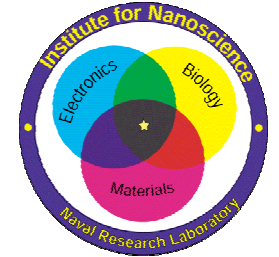
A New *Air-Stable* Electron Transport Material

- Demonstrated non-dispersive “trap-free” and fast electron transport
- Measured high electron mobility in air
- Two orders of magnitude larger than that of Alq₃

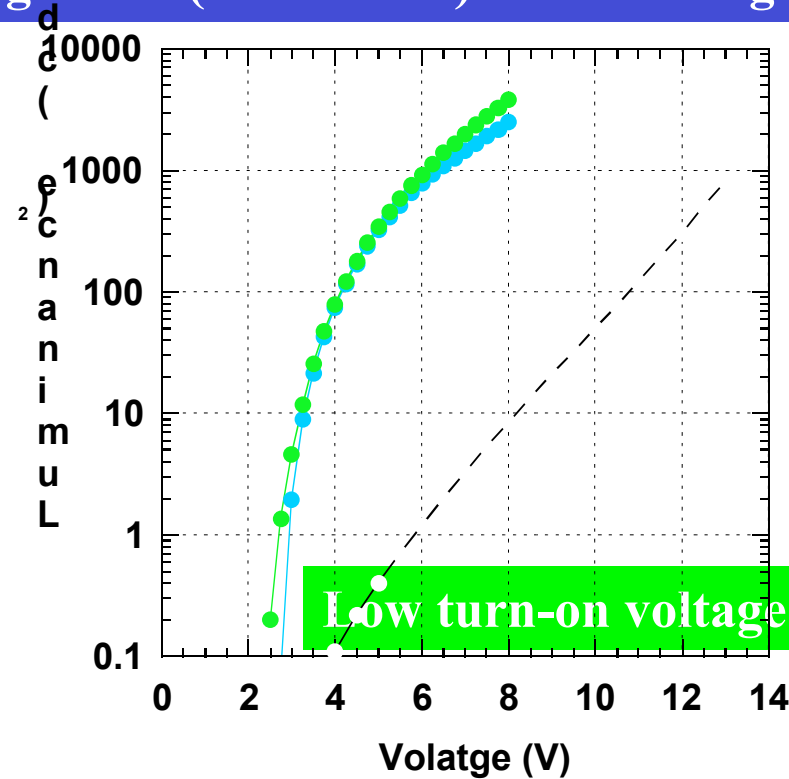
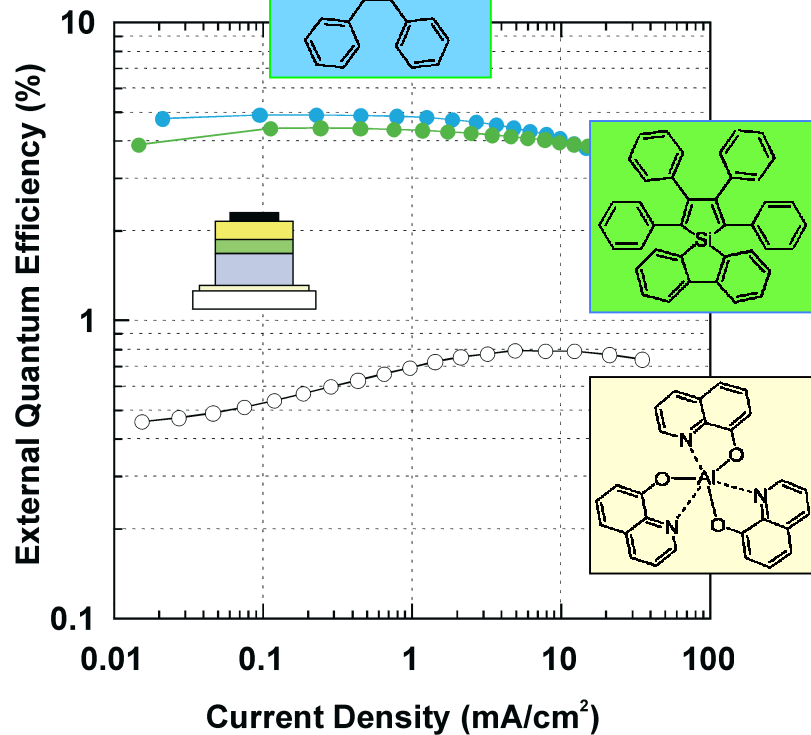
Murata, Malliaras, Uchida, Shen, Kafafi, Chem. Phys. Lett. 339, 161 (2001)



Highly-Efficient Electroluminescent Devices Based on Silole Derivatives



High brightness (4000 cd/m²) at low voltage (8V)

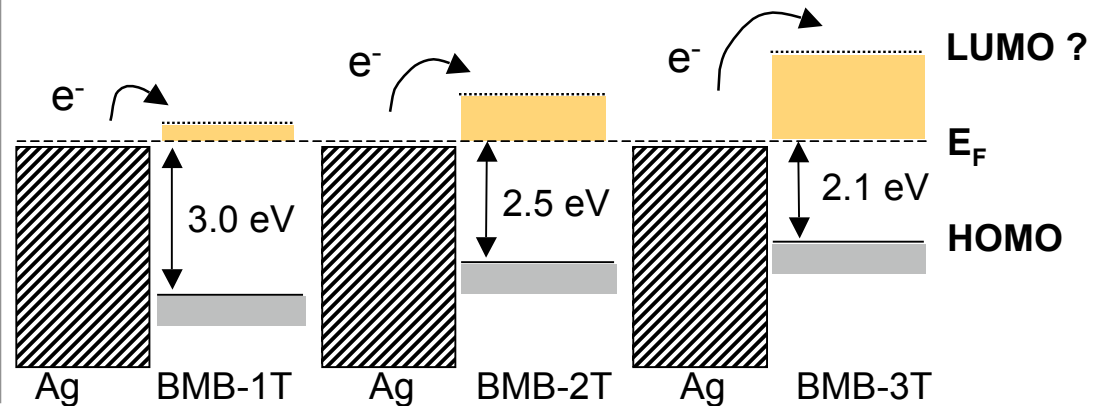
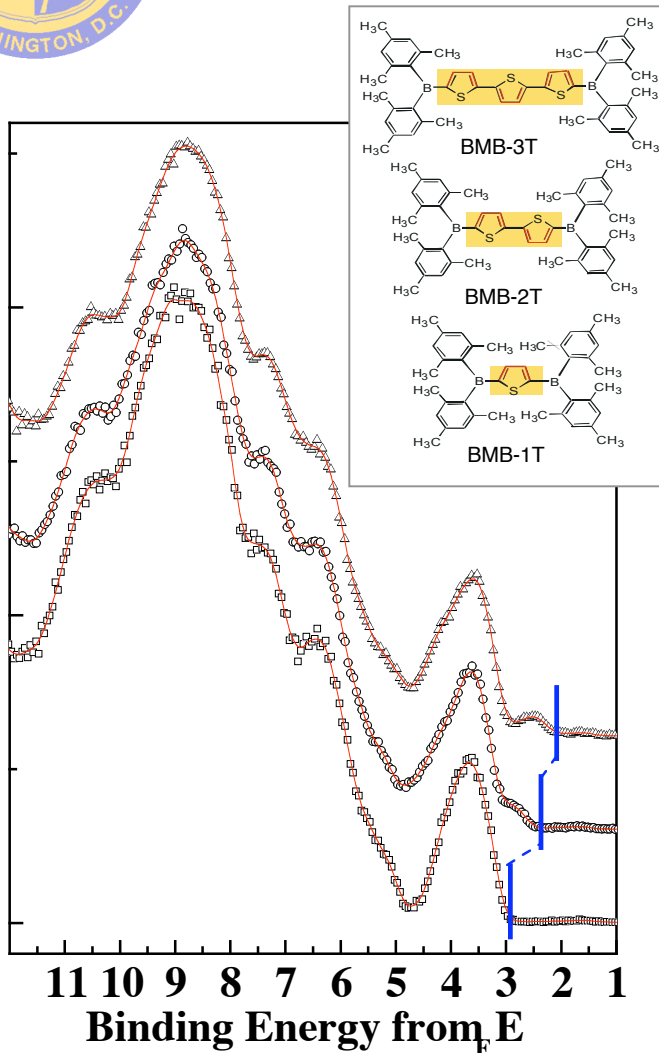
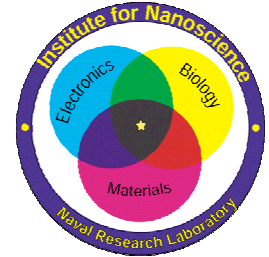


EL quantum efficiency close to the theoretical limit!

Murata, Uchida, Kafafi, Appl. Phys. Lett. 80, xx (2002)



Energy Levels Alignment at Metal/BMB-nT Interfaces



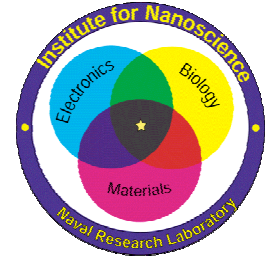
- Determined barriers to hole (E_{h^+}) injection
- Estimated barrier to electron (E_{e^-}) injection
- Showed that E_{h^+} decreases and E_{e^-} increases as a function of the π electron delocalization length (number of thiophene rings)

BMB-1T is the best electron transporter

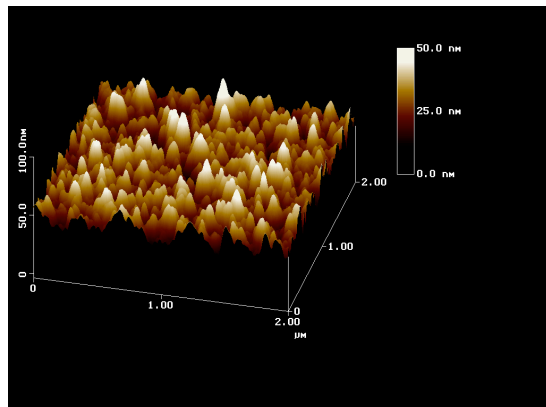
Mäkinen, Shirota, Kafafi, et al. Appl. Phys. Lett. 78, 670 (2001)



AFM Pictures of Transparent Electrodes Grown by PLD on Plastics

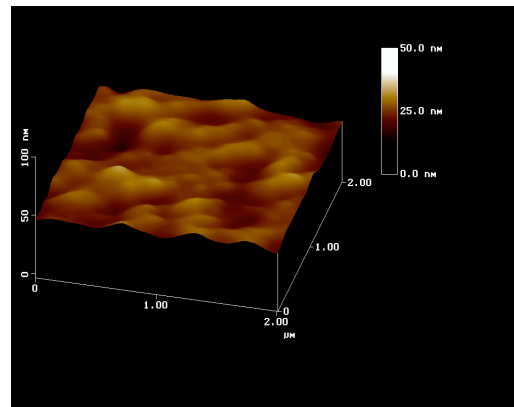


Bare PET



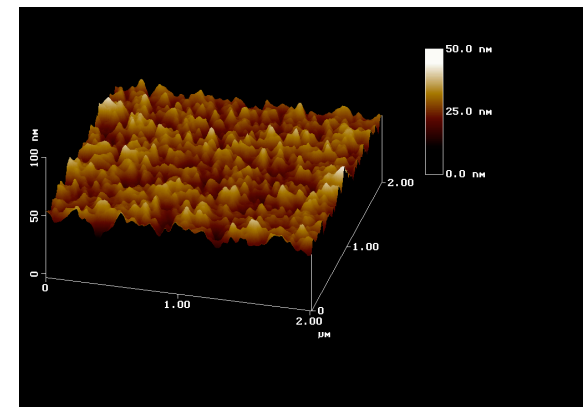
- RMS roughness: 8-10 nm

ITO on PET



- RMS roughness: 2-3 nm
- Transmission: 80%
- Work function: 4.5 eV

AZO on PET



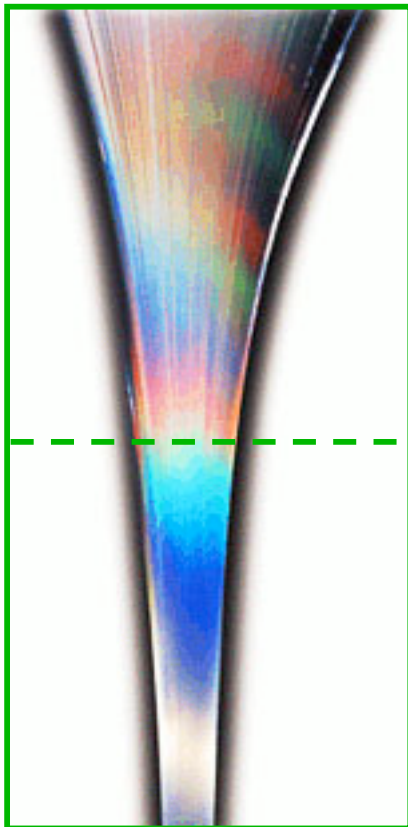
- RMS roughness: 3 nm
- Transmission: 80%
- Work function: 4.0 eV

- PLD TCO films planarize substrate and reduce surface roughness
- AZO is a good candidate for transparent cathode due to low WF

H. Kim *et al.*, APL 79, 284 (2001)



2D Photonic Crystals



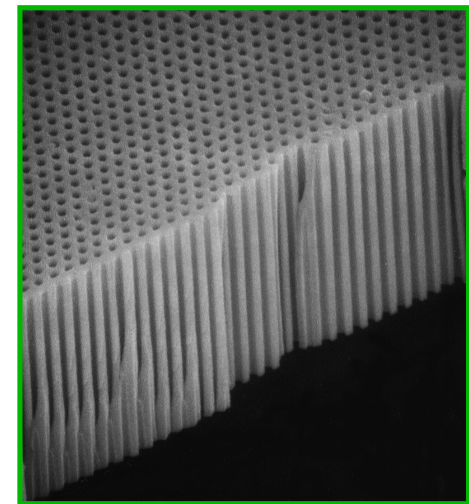
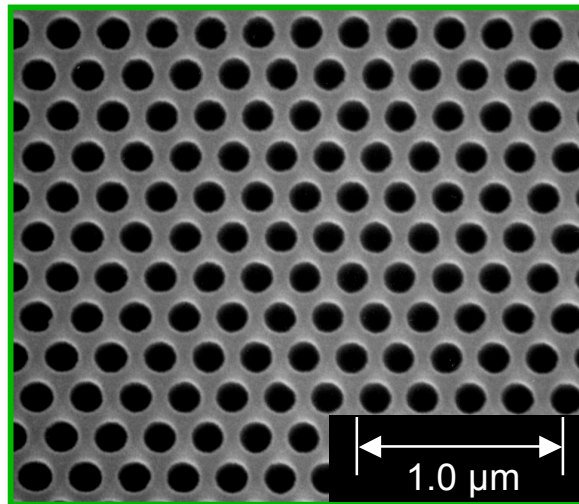
A composite glass material:

fabricated as a regular array of glass cylinders in a glass matrix

after wet etch: array of holes in a glass matrix

length scale of array is $\sim \lambda$ of light

⇒ *Prototypical 2D photonic crystal*



R.J. Tonucci, B.L. Justus, A.J. Campillo,
and C.E. Ford, *Science* 258, 783 (1992)

- Typical for this composite glass:
- Hole diameter: $\sim 5 \mu\text{m}$ to $\sim 30 \text{ nm}$
 - Triangular lattice, $a \sim 3r$
 - $\sim 10^7$ elements in a wafer

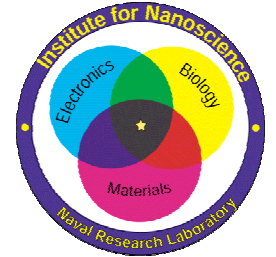
*Photonic Band
Gap Materials*

Armand Rosenberg
NRL Code 5613
202-767-9522

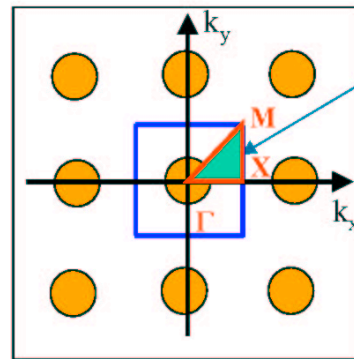


2D Photonic Band Structure

Examples

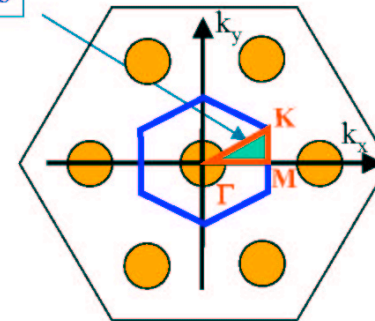
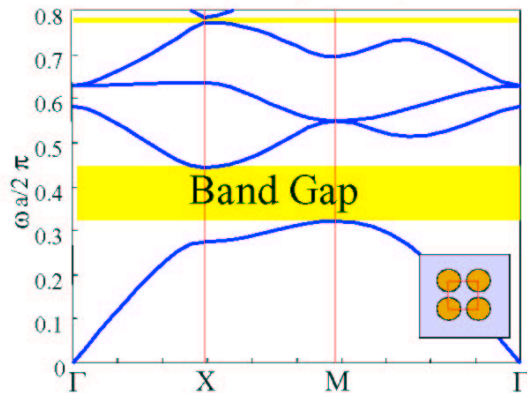


holes in $\epsilon=9$,
 $r=0.2a$



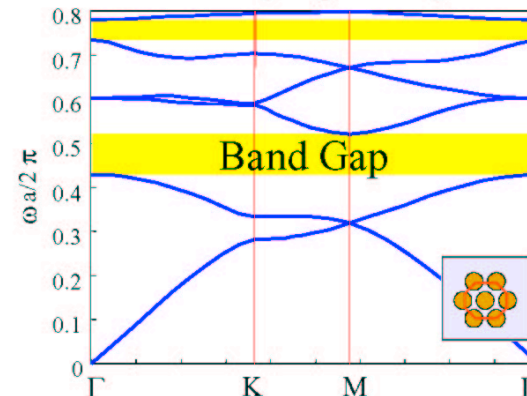
Irreducible Brillouin Zones

TM mode (Rectangular lattice)



holes in $\epsilon=13$,
 $r=0.5a$

TM mode (Triangular Lattice)



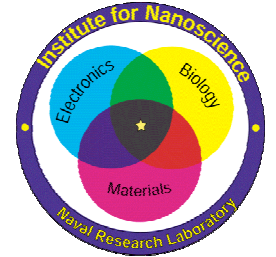
Objective: decoupling of the electronic and optical properties...

- Electronic band structure arises from the intrinsic material properties [*scale: $\sim 1 \text{ \AA}$*]
 - Photonic band structure arises from structural control (patterning) of the material [*scale: $\sim \lambda$ of light*]
- ⇒ combinations of optical/electrical properties unavailable in nature

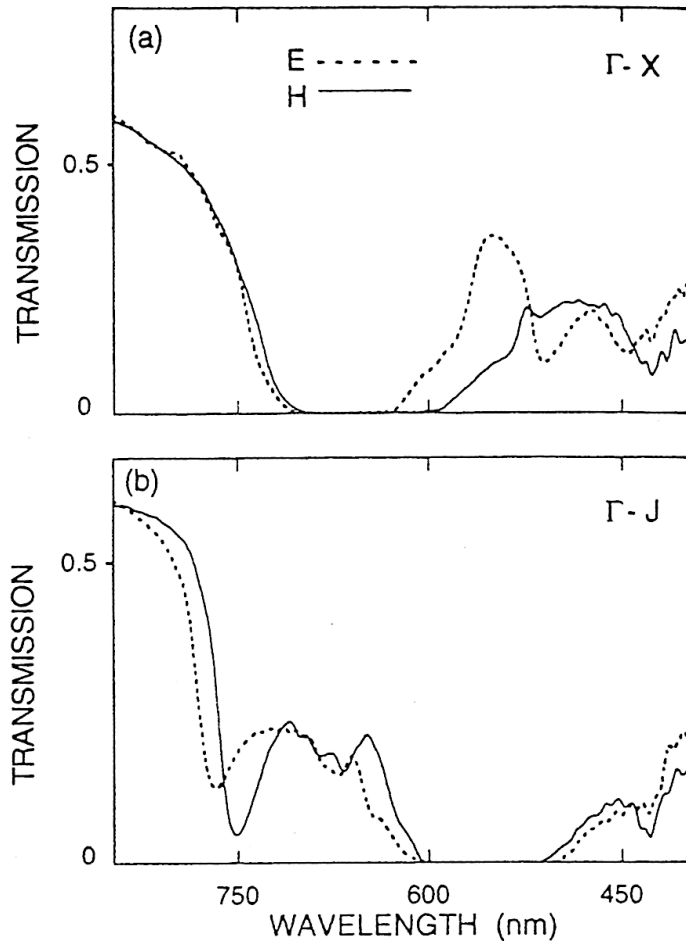


Observation of 2D Photonic Band Structure

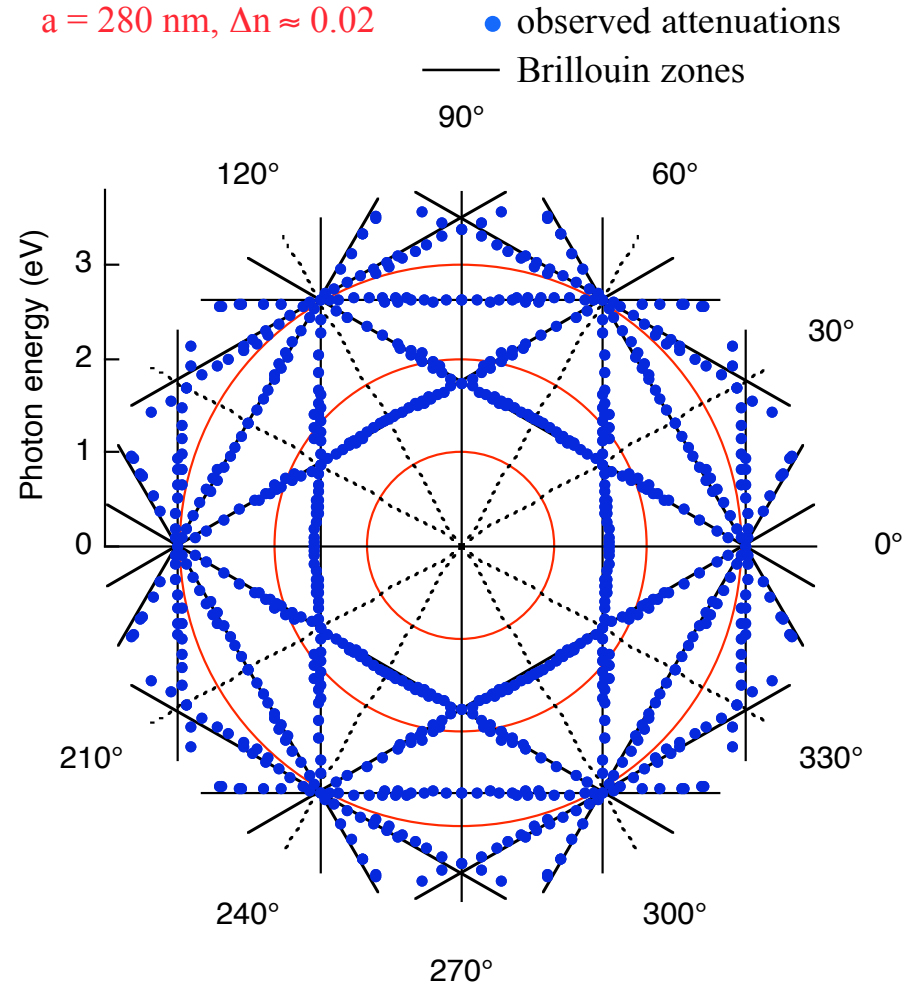
First experimental demonstration of 2D photonic band gap effects in the visible/near-IR based on NRL's composite glass



$a = 220 \text{ nm}$, $\Delta n \approx 0.45$



$a = 280 \text{ nm}$, $\Delta n \approx 0.02$

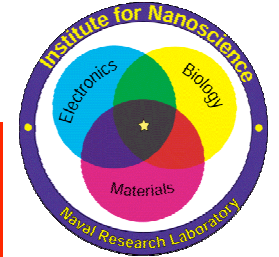


H.B. Lin et al., Appl. Phys. Lett. 68, 2927 (1996)

A. Rosenberg et al., Appl. Phys. Lett. 69, 2638 (1996)

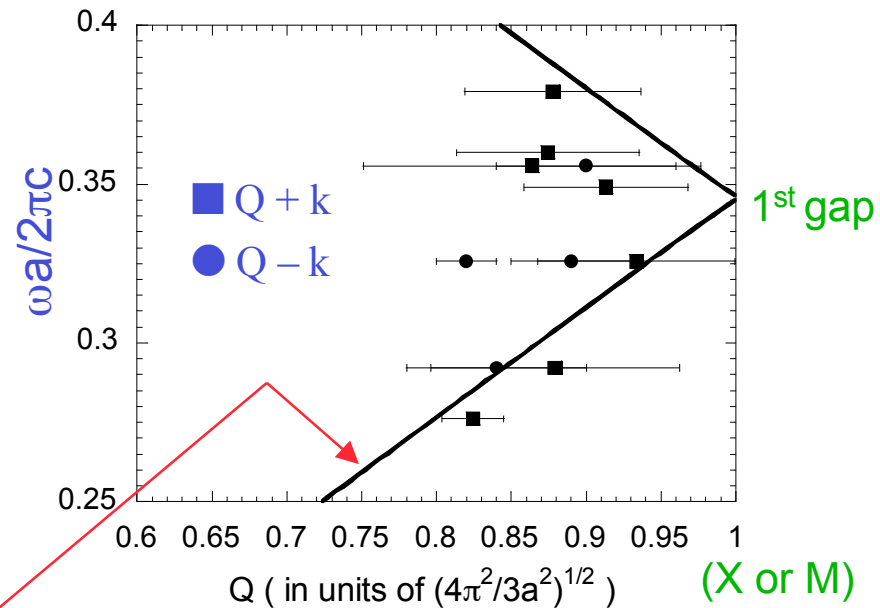
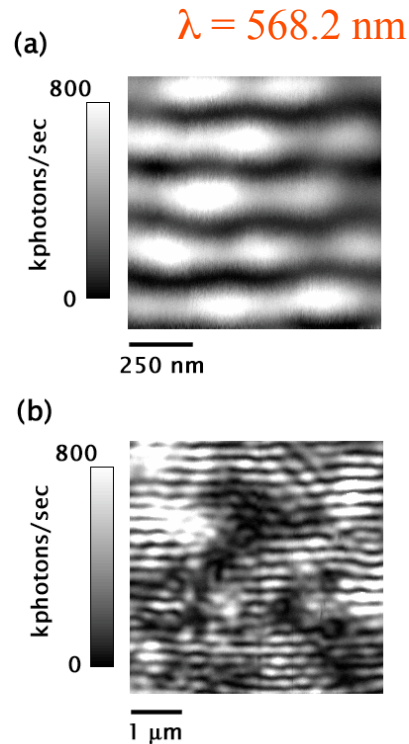


NSOM Studies of PBG Properties



First direct mapping of the spatial distribution of optical intensity within a 2D PBG structure based on NRL's composite glass

- NSOM probes the evanescent field of light propagating in a 2D PBG structure
- Results below are for glass cylinders in a glass matrix (small index contrast)
- Probe tip perturbs field at higher index contrast



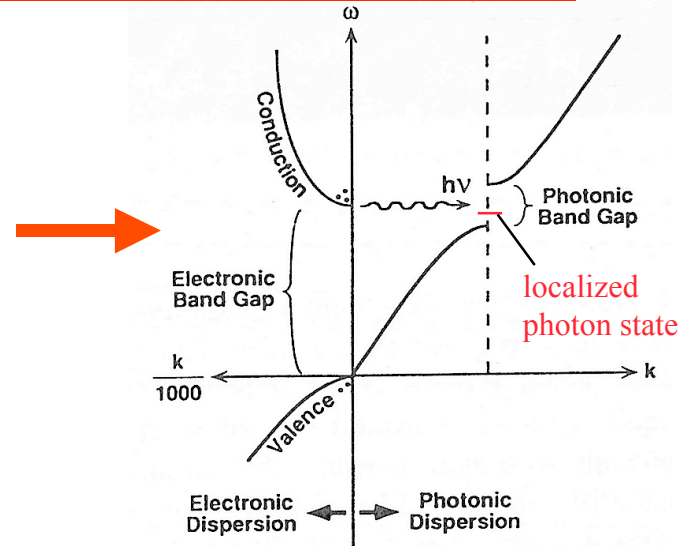
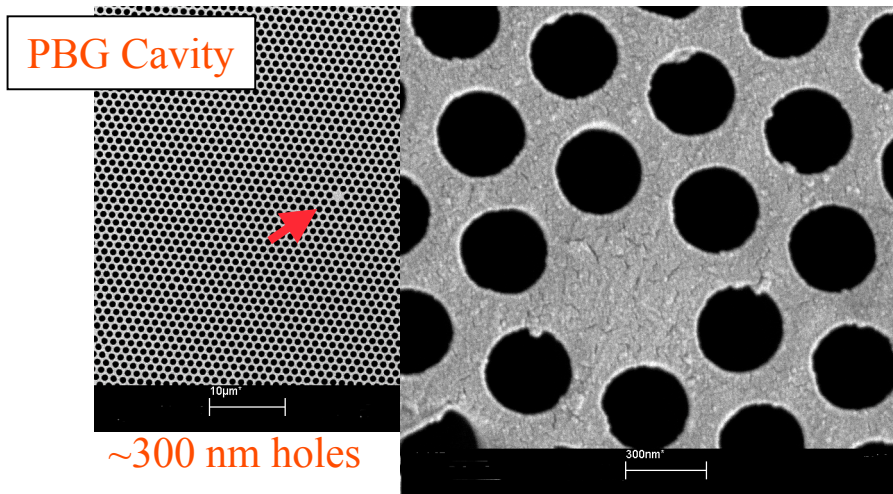
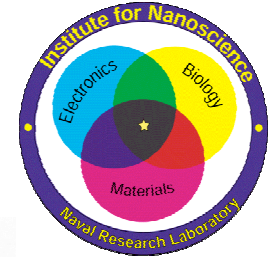
Calculation: $n_{\text{cyl}}=1.68$, $n_{\text{matrix}}=1.66$, $a=185 \text{ nm}$, $d_{\text{cyl}}=135 \text{ nm}$
no adjustable parameters

A.L. Campillo et al., J. Appl. Phys. 89, 2801 (2001)

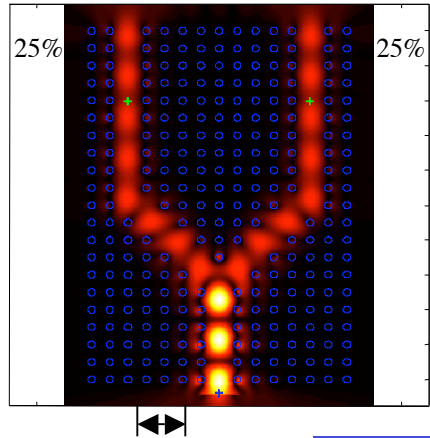


PBG Optoelectronic Components

Objective: Demonstrate miniaturized optoelectronic devices based on PBG components

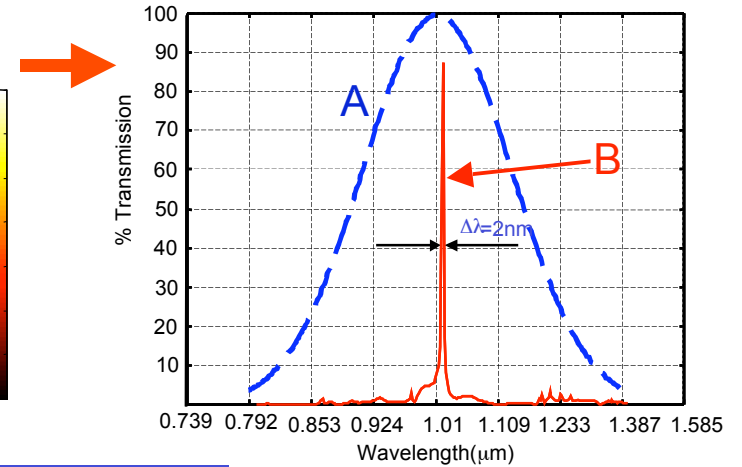
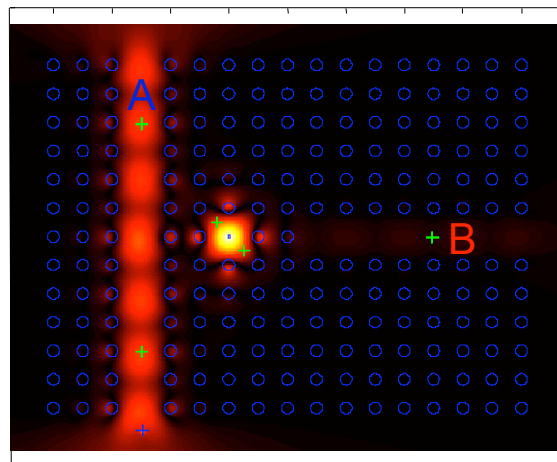


PBG Channel Waveguides with Sharp Bends (Splitter)



scale: $\sim \lambda$

PBG Cavity + Channels (Add/Drop Filter)



A. Sharkawy, S. Shi, D.W. Prather, Applied Optics, 40, 2247 (2001)



Future PBG Optoelectronic Devices based on GaN

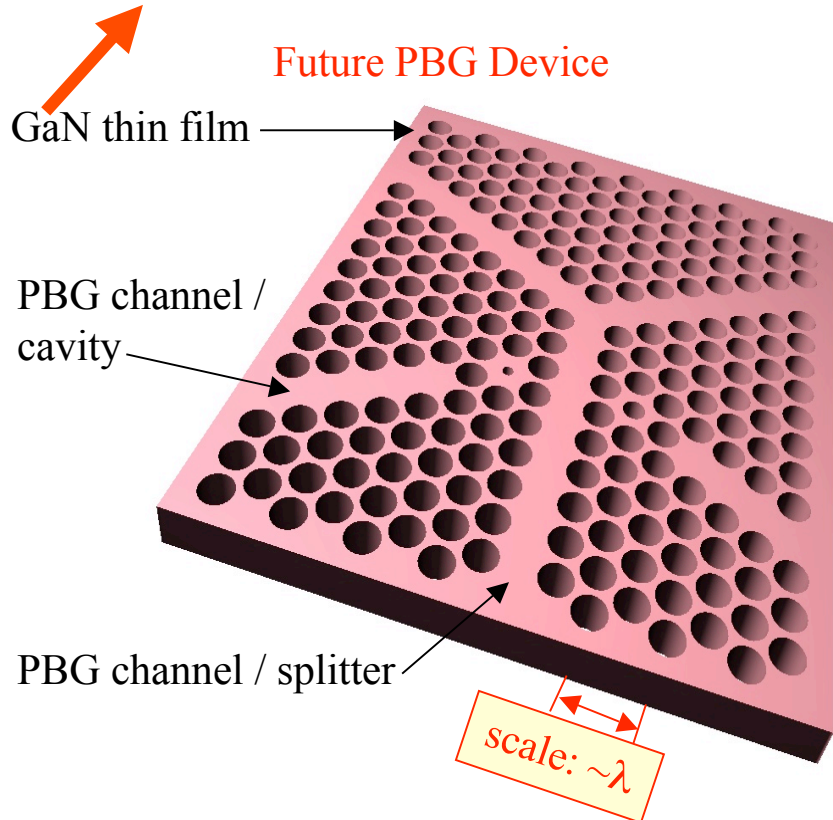
GaN is a “new” material: requires process development



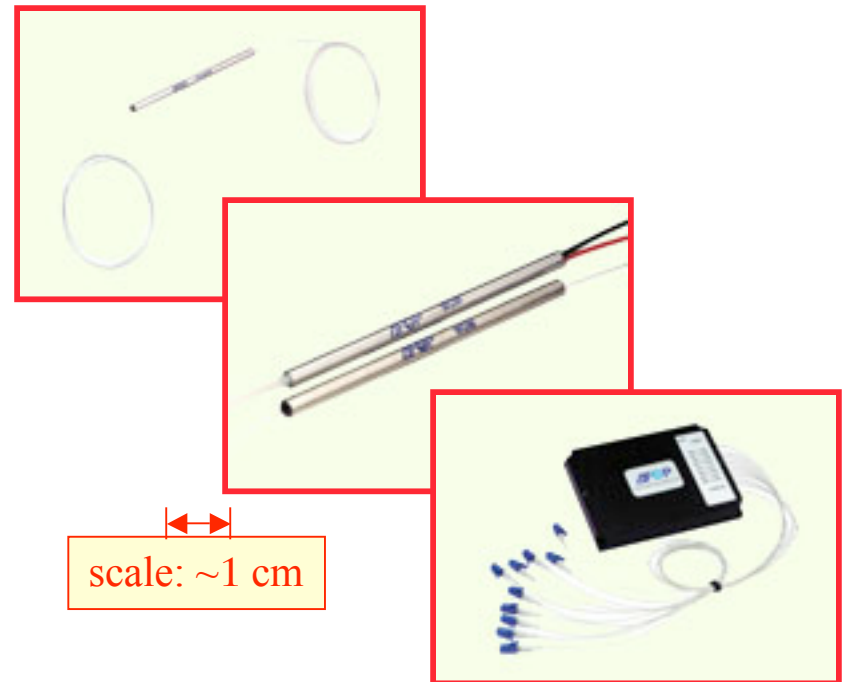
Approach: Fabricate 2D PBG patterns in wide-band semiconductor planar waveguide

Initial goal: Demonstration of PBG components in GaN

One of the highest refractive indices in a material that is transparent throughout the visible and infrared



“vs”

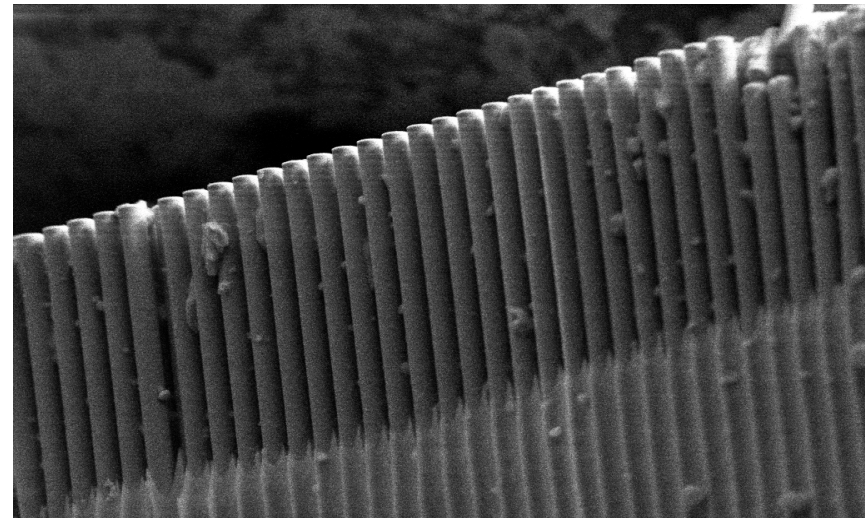
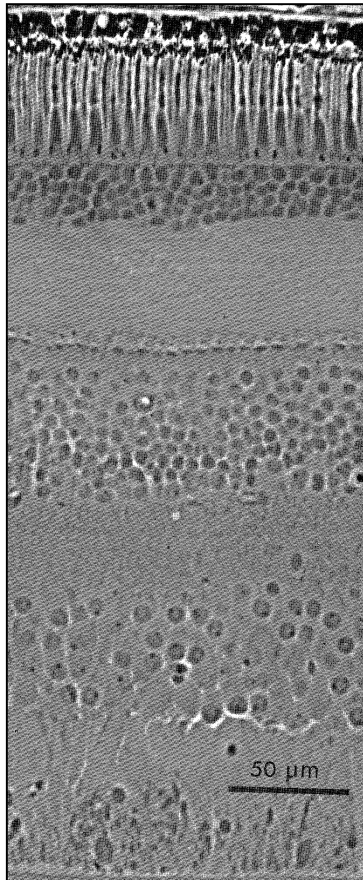




Neural-Electronic Interfaces



Principal Investigator: Dean Scribner (scribner@nrl.navy.mil)
co-PI: Brian Justus (justus@nrl.navy.mil)

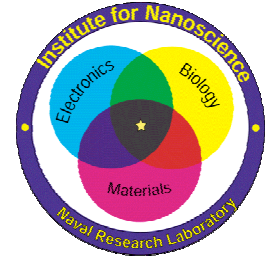


Objectives:

- **Develop a large, dense bio-electronic interface array for communicating with neural tissue**
- **Learn how biological tissue processes information on a massive, parallel scale**



Nanochannel Glass Microelectrode Arrays



Nano-channel glass technology enables connections to millions of neurons

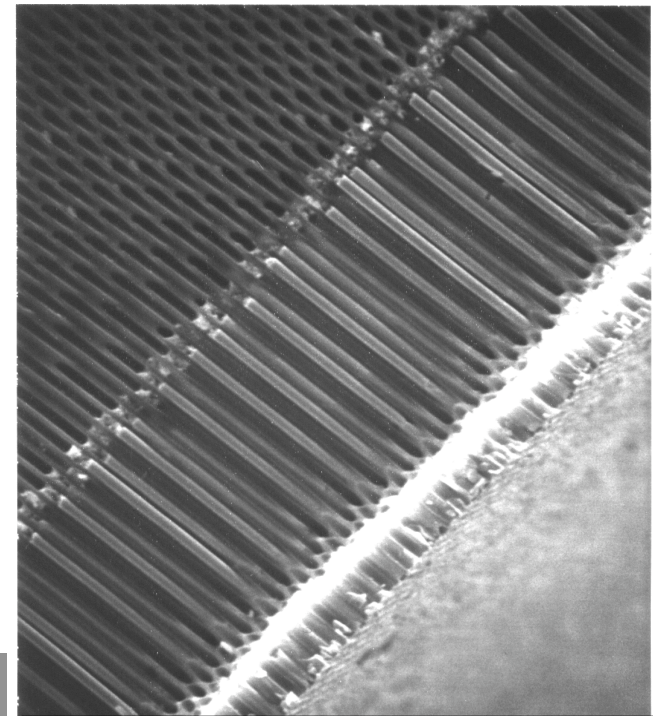
Advantages:

- **Compatible with biological tissue**
- **Conformable to curvature of any neural surface**
- **Uniform array of millions of metal electrodes**
- **Micro-nanometer scale spatial resolution**

Current features:

- **Small electrodes ($D = 5.5 \mu\text{m}$)**
- **Large array area ($> 1 \text{ cm}^2$)**
- **No channel cross-talk**

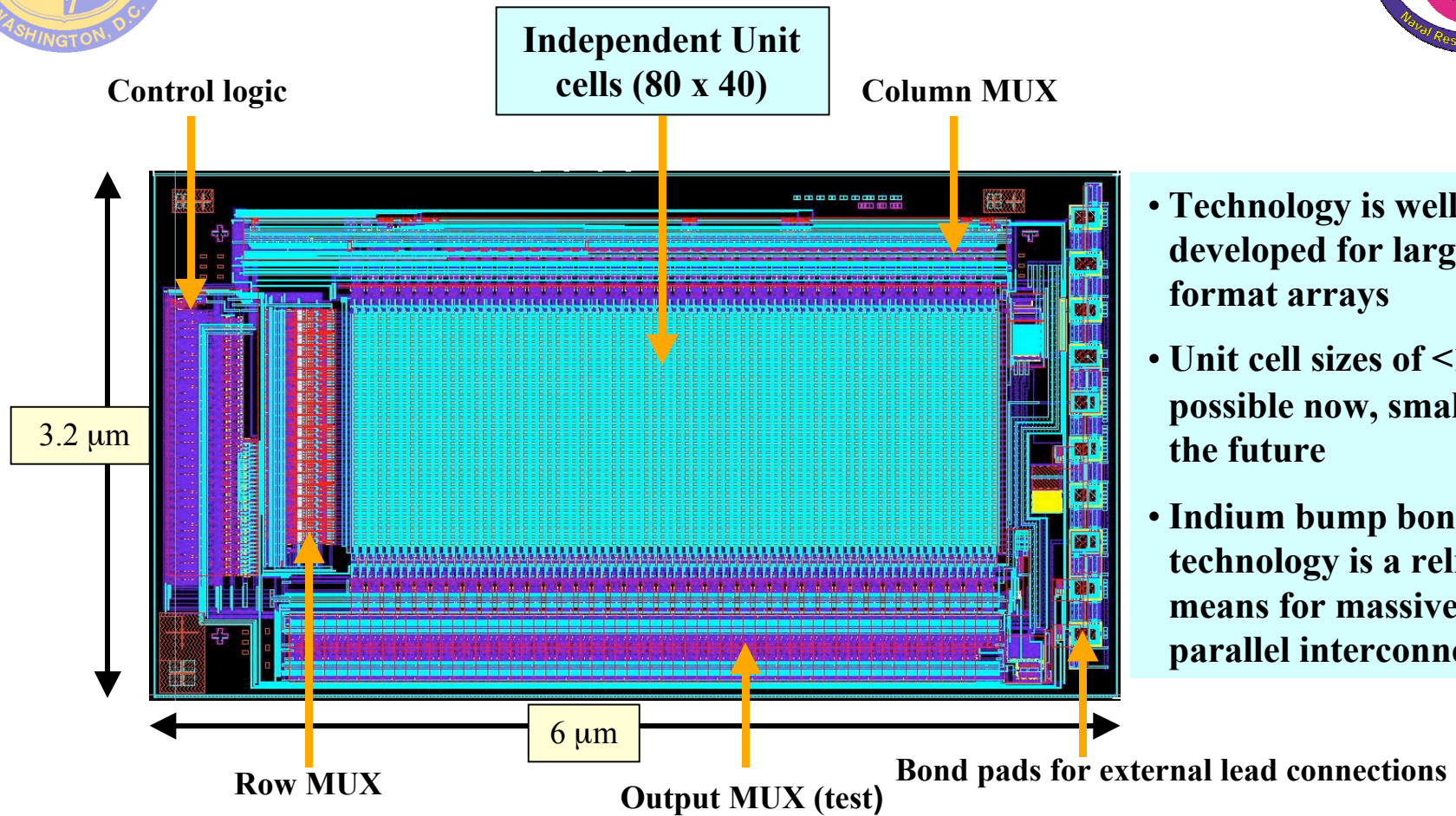
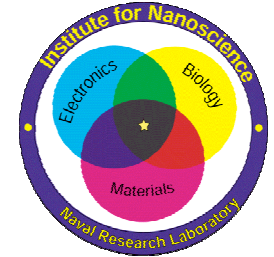
NRL Nano-channel glass technology is capable of providing large, parallel arrays of small, high aspect ratio conductors



Electro-deposited Pt wires



2-D Multiplexer Arrays

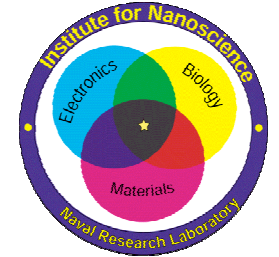


- Technology is well developed for large 2-D format arrays
- Unit cell sizes of $<15 \mu\text{m}$ possible now, smaller in the future
- Indium bump bond technology is a reliable means for massive parallel interconnections

Multiplexer connects thousands of neural sites to outside world via a handful of external leads

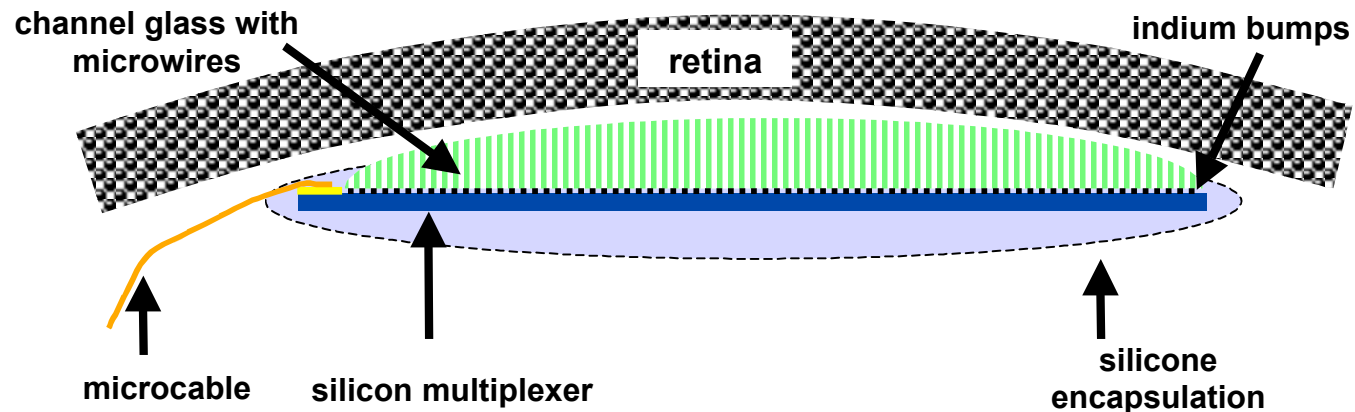


A Model Neural-Electronic Interface: Artificial Retinal Stimulation



Ultimate goal is to restore visual capabilities to patients with retinitis pigmentosa and macular degeneration affecting >10 million people in U.S.

The nanochannel glass will allow for a curved surface with low impedance

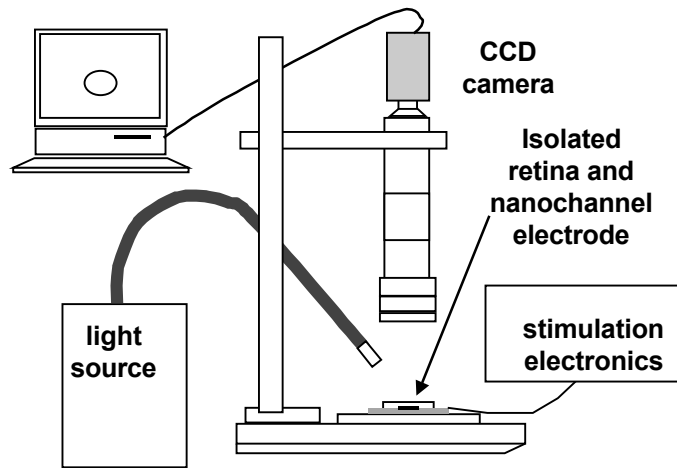
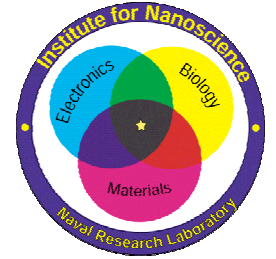


Combining nano-channel glass and silicon multiplexer technologies provides a powerful new approach for simultaneously addressing thousands of neurons



Neural Computation in Biological Systems

What Can we Learn & Apply to Navy Sensors?



A retinal imaging system

The areas of the retina stimulated by the electrode will appear as regions of increased brightness



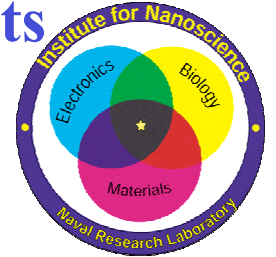
A movie of electrical potential changes. After mechanical stimulation (arrow) the system detects a change in the retina light scatter. In this example a "wave" of potential change moves across the retina.



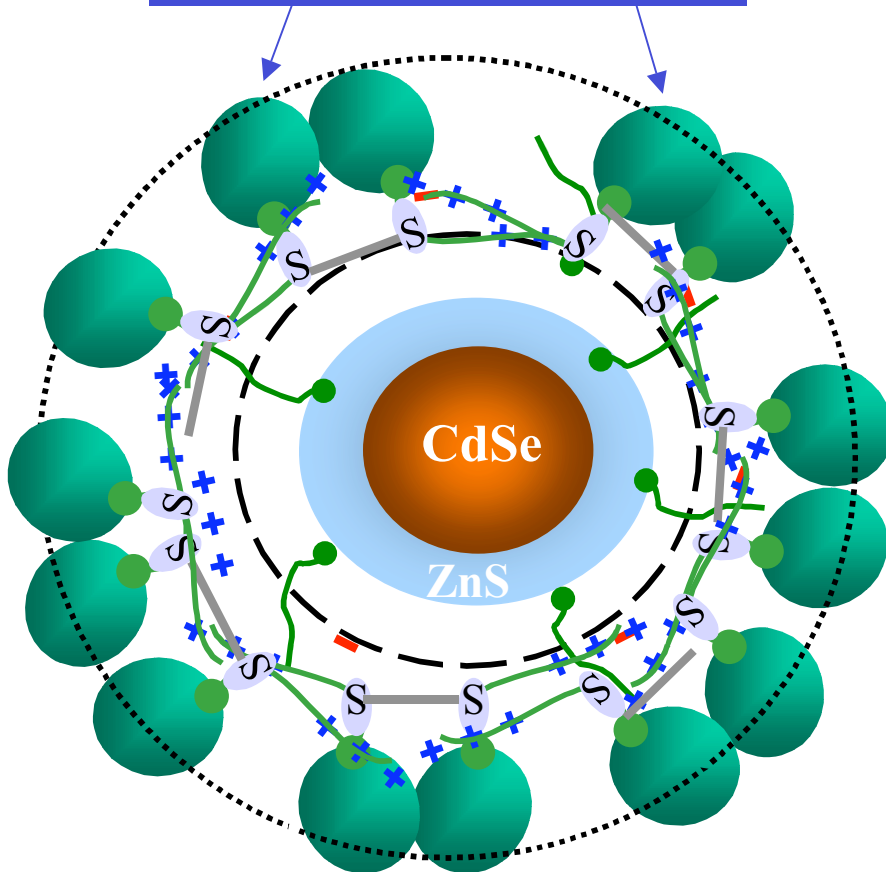
Biologically Conjugated Luminescent Quantum Dots

Hedi Mattoussi and Brian Justus

Phone: 202-767-9473; Email: hedimat@ccs.nrl.navy.mil



Maltose binding protein

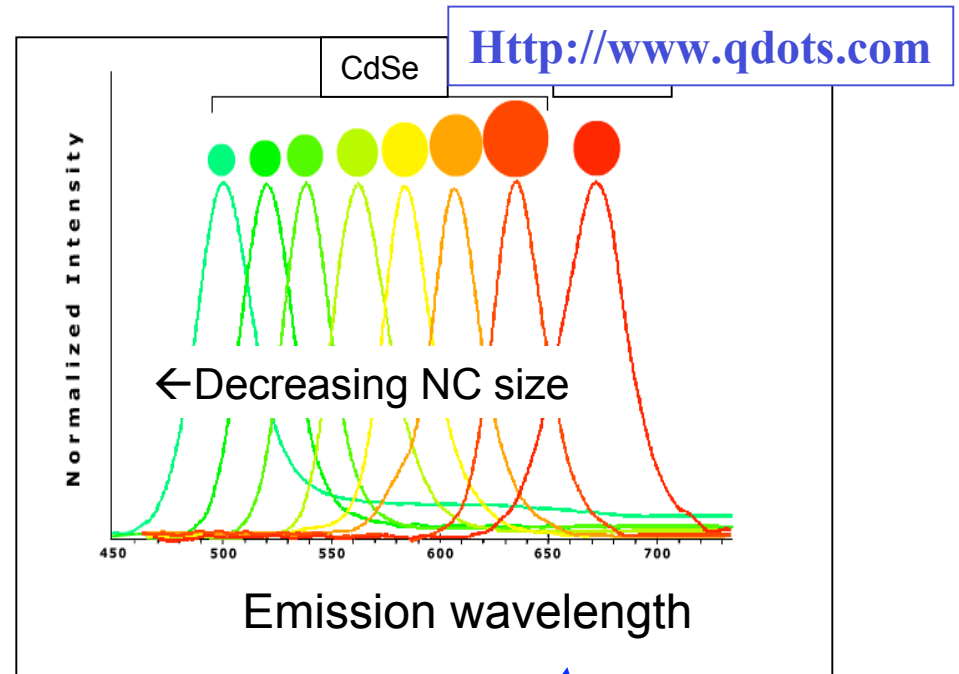
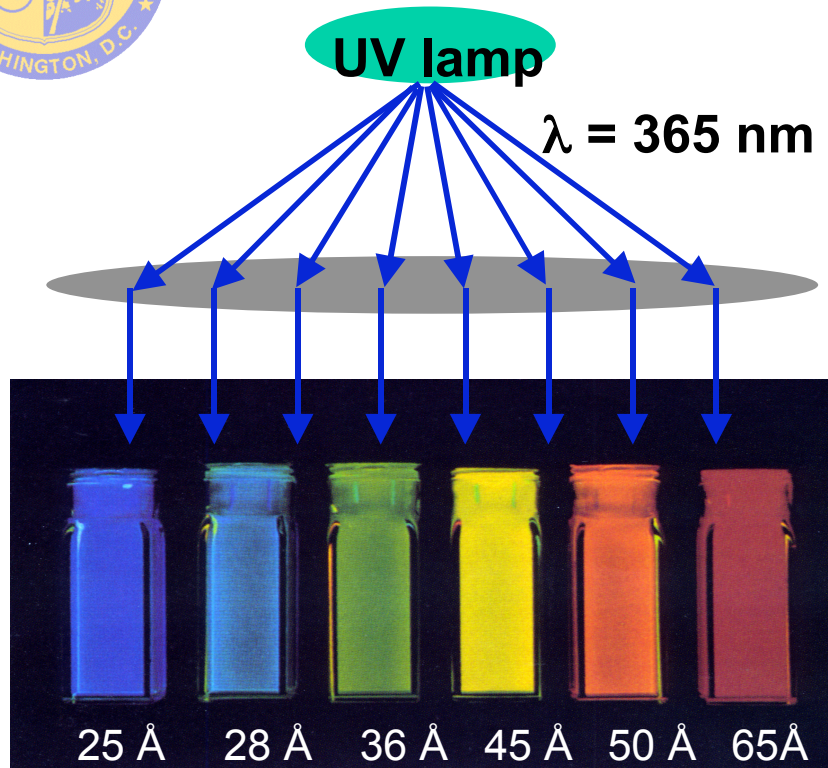
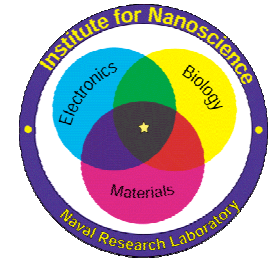


Objectives:

- Develop novel semiconducting nanocrystals that are both luminescent and biologically active
- Develop ultrasensitive detection of chemical and biological materials via these luminescent quantum dot bioconjugates.

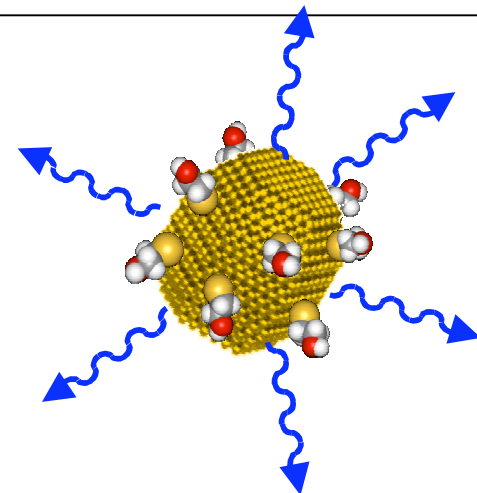


Luminescent Nanocrystalline Particles



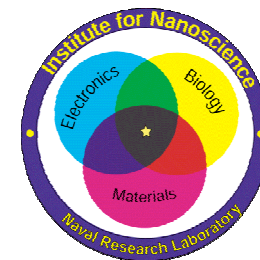
- Control of nanocrystal size
- Solution phase synthesis
- Size selective precipitation
- Capping layers
- Tunable band gaps

B.O. Dabbousi, et al., *J. Phys. Chem.* **101**, 9463 (1997)





Electrostatically Driven Self-Assembly of Quantum Dot Bioconjugates

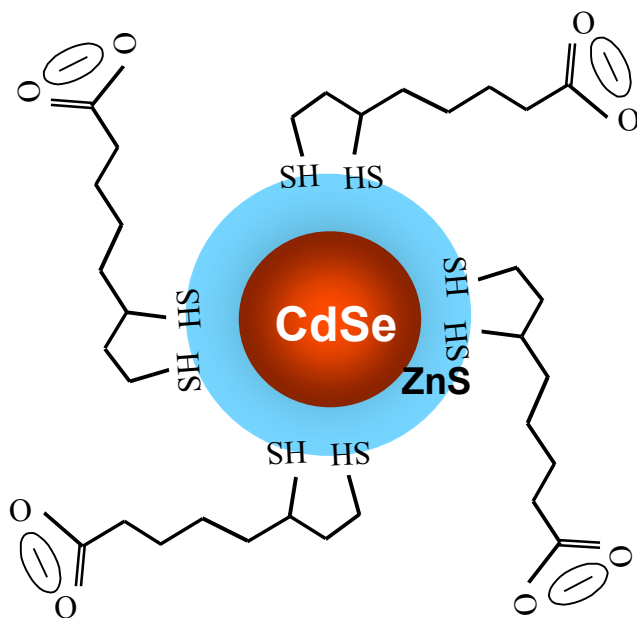


Negatively charged, lipoic acid-capped nanocrystal

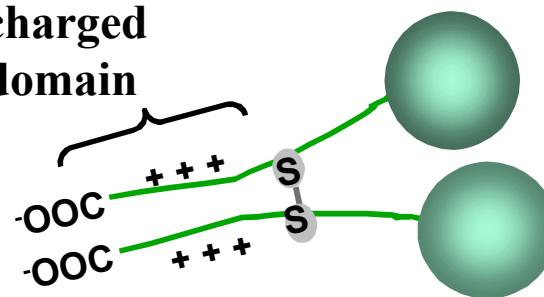
Electrostatic

attraction

Positively charged, 2 domain protein



Positively charged domain

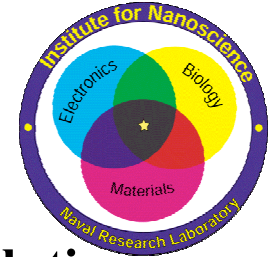


Biologically active domain

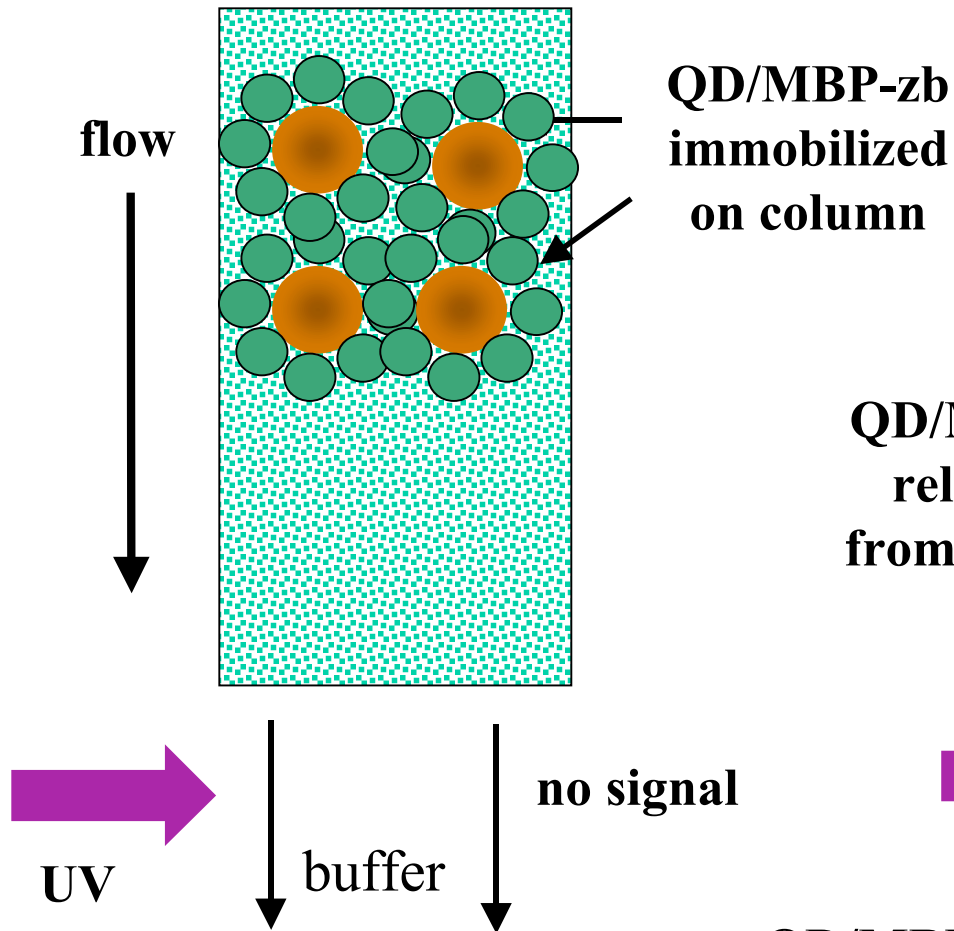
H. Mattoussi et al. *J. Am. Chem. Soc.*, 122, 12142 (2000)



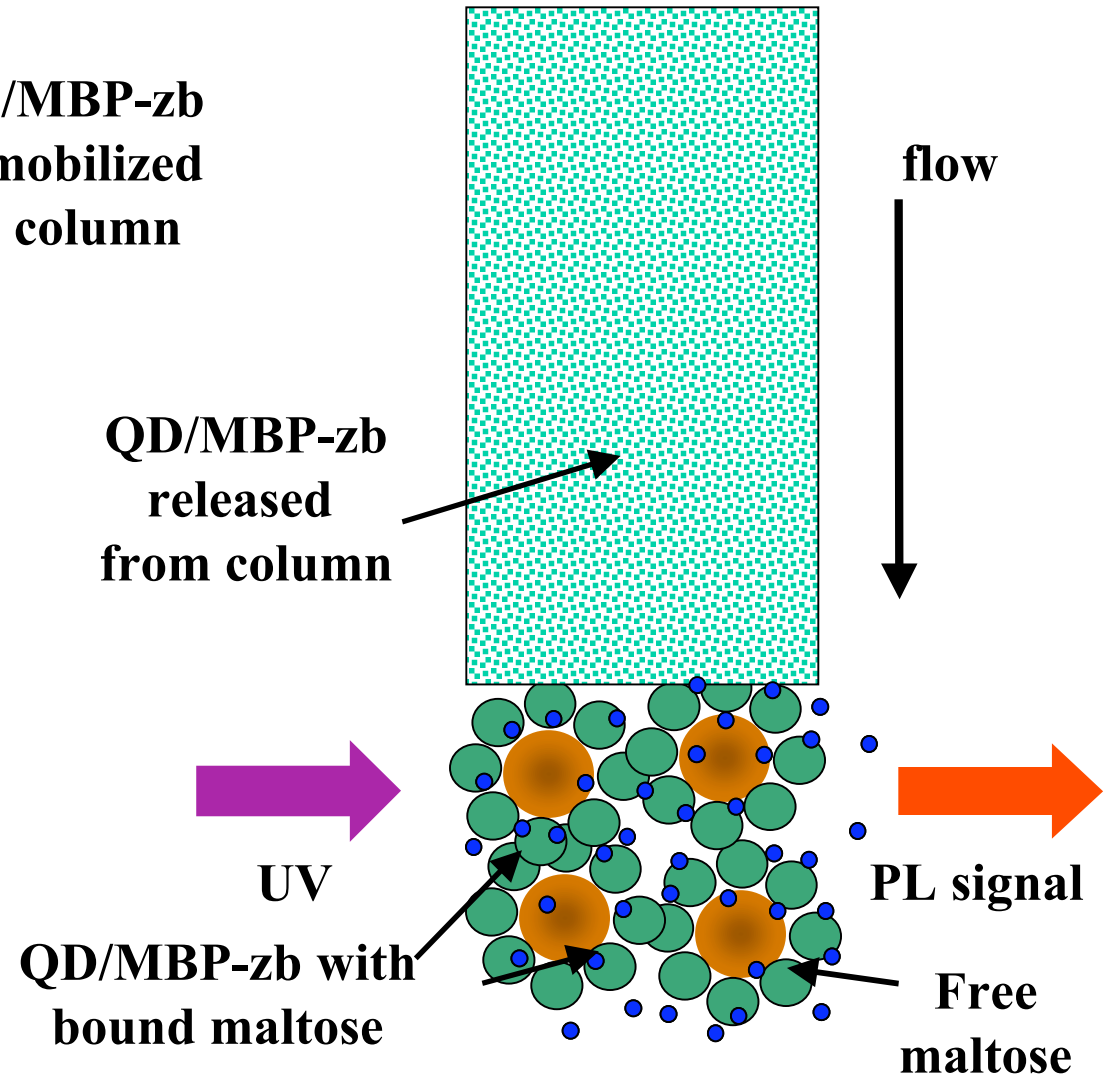
Maltose binding protein (MBP): Fluorescence assay for maltose

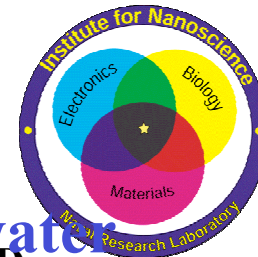


I. Amylose resin in column

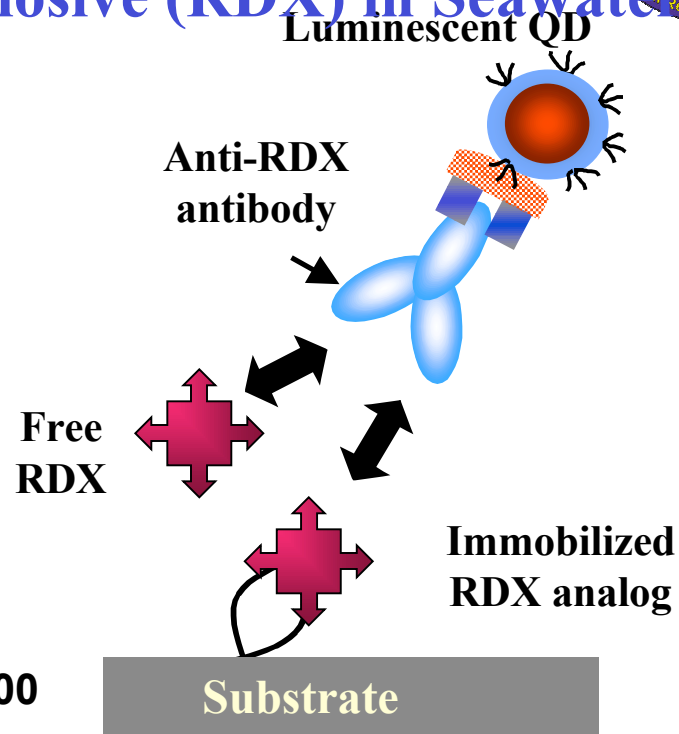
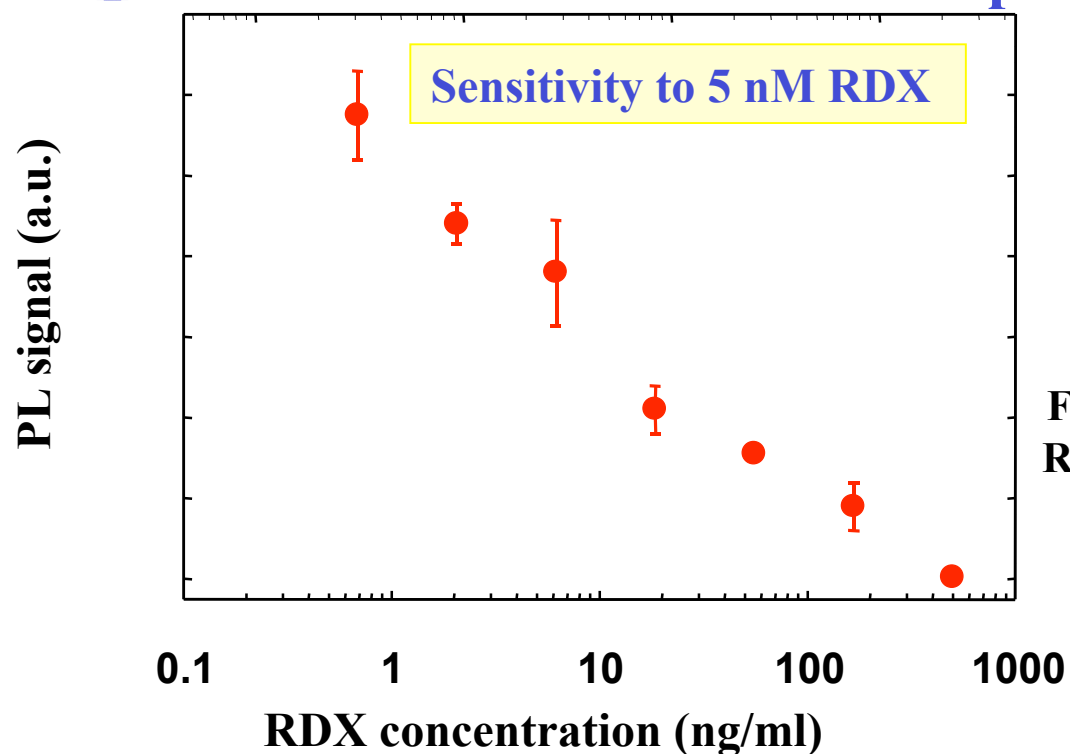


II. Inject maltose solution





Detection of Trace Levels of Explosive (RDX) in Seawater



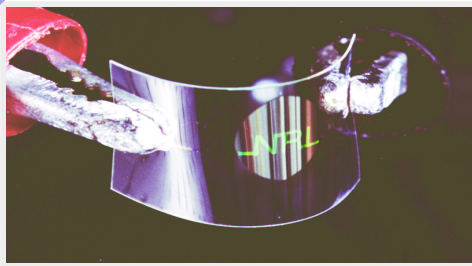
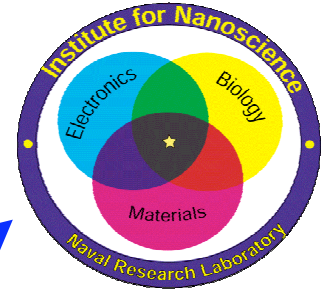
Competition Assay

- Prepare QDs conjugated with anti-RDX antibodies
- Measure PL of QD-bioconjugates bound to a surface prepared with RDX analogs
- Free RDX competes for bioconjugate and reduces PL signal

E. R. Goldman, in press, *Analytical Chemistry* (2001)



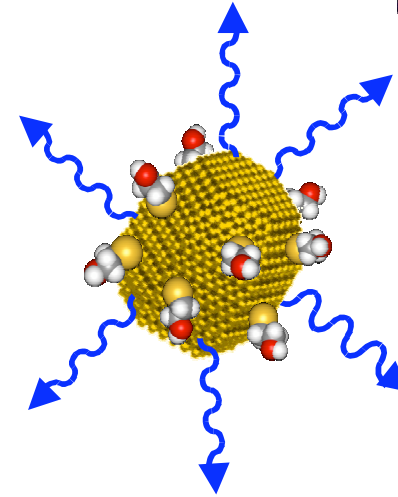
NANOSCIENCE RESEARCH IN OPTICS



Organic Light-Emitting Materials & Devices

Zakya Kafafi

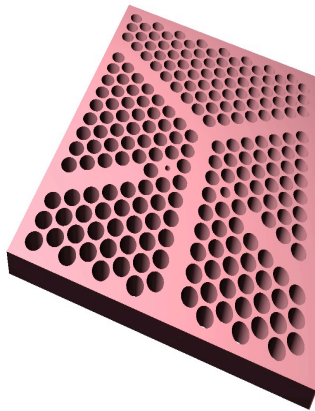
(kafafi@ccf.nrl.navy.mil)



Biologically Conjugated Luminescent Qdots

Hedi Mattoussi (hedimat@ccs.nrl.navy.mil)

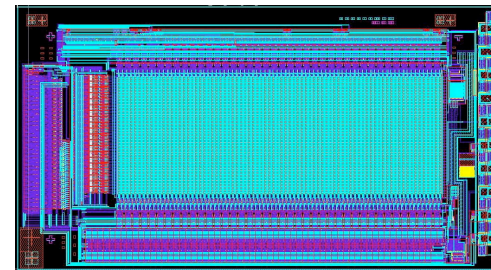
Brian Justus (justus@nrl.navy.mil)



2D Photonic Crystals

Armand Rosenberg

(Armand.Rosenberg@nrl.navy.mil)



Neural Electronic Interfaces

Dean Scribner

(scribner@nrl.navy.mil)